Contents lists available at AccScience Publishing
Nonlinear Science and Control Engineering (NSCE)
Vol. 1, No. 2 (2025)
https://accscience.com/journal/nsce

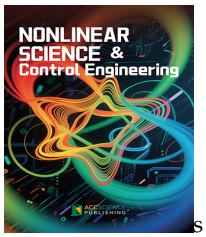

An analytical investigation of the wave propagation behavior of the truncated M-fractional Landau–Ginzburg–Higgs model through two consent techniques

M. Al Amin[1]*, M. Nurul Islam[1], M. Ali Akbar[2]

[1]*Department of Mathematics, Faculty of Sciences, Islamic University, Kushtia, Khulna, Bangladesh*
[2]*Department of Applied Mathematics, Faculty of Science, University of Rajshahi, Rajshahi, Bangladesh*

Article History:
Received: July 20, 2025
Revised: September 17, 2025
Accepted: October 9, 2025
Published online: November 14, 2025

ABSTRACT

The nonlinear fractional Landau–Ginzburg–Higgs (LGH) model is a renowned nonlinear integrable mathematical model that is used to explain the nonlinear signal that shows weak scattering and radial links in the tropical and mid-latitude troposphere as interplays between equatorial and mid-latitude Rossby waves, superconductivity, and drift cyclotron waves in radially inhomogeneous plasma for coherent ion-cyclotron waves and equivalent incidents. This article investigates the fractional order of the LGH model utilizing two recent schemes: the generalized exponential rational function method and the extended tanh-function method, incorporating the truncated M-fractional derivative.Using these methods, we obtained a large number of different types of traveling wave solutions, including exponential functions, hyperbolic functions, trigonometric functions, rational functions, and their composite functions. Moreover, we examined the influence of wave velocity parameters on the soliton by sketching three-dimensional, along with two-dimensional plots of the obtained results. The attainment outcome authenticates the effectiveness and consistency of the utilized methods. The appropriateness of the obtained solutions is settled by putting them into their original model.

Keywords: Extended tanh-function method; Generalized exponential rational function method; Nonlinear fractional Landau–Ginzburg–Higgs (LGH) model; Soliton solution; Truncated M-fractional derivative

1. Introduction

The physical phenomena that arise in our real-world applications are generally expressed in mathematical form using nonlinear partial differential equations (PDEs). There is a special type of nonlinear PDEs known as nonlinear evolution equations (NLEEs). The NLEEs have a broad range of applications in various domains,

***Corresponding author**:
M. Al-Amin (m.alamin.iu@gmail.com).

Citation:
Al Amin M, Nurul Islam M, Ali Akbar M. An analytical investigation of the wave propagation behavior of the truncated M-fractional Landau–Ginzburg–Higgs model through two consent techniques. *Nonlinear Sci Cont Eng.* 2025;1(2):025290004. doi: 10.36922/NSCE025290004

including mathematics, physics, science, and other fields,such as optical physics, atomic physics, chemically dispersed electricity, plasma physics, solid-state physics, hydrodynamics, geo-optical filaments, nuclear physics, and fluid mechanics. The solitary wave solution of NLEEs carries important physical information and supplementary understanding about the problem. As a result, the solutions of NLEEs have become a burning issue in the current age.

Researchers have derived a variety of well-organized definitions and solution techniques of the nonlinear fractional PDEs, such as, truncated M-fractional derivative (TMFD),[1] Caputo–Fabrizio,[2] beta-derivative,[3] conformable derivative,[4] and the solution techniques include generalized exponential rational function (GERF) technique,[5] modified sub-equation technique,[6] auxiliary equation scheme,[7–9] modified simplest equation technique,[10] Sardar sub-equation technique,[11] residual power series scheme,[12] Hirota N-soliton conditions technique,[13–16] extended tanh function approach,[17] method of $m+(G'/G)$-expansion,[18] $(G'/G,1/G)$-expansion scheme,[19,20] inverse scattering transformation scheme,[21] Nucci's reduction technique,[22] Hirota bilinear and tri-linear formation scheme,[23] improved F-expansion scheme,[24] improved generalized Riccati equation mapping technique,[25] exp_{a} function scheme,[26] method of B-spline,[27] method of $(1/G')$-expansion,[28] generalized (G'/G)-expansion scheme,[29,30] logarithmic transformation technique,[31] Binary Darboux transformations technique,[32] etc.

In the meantime, scholars have derived numerous models to explain various physical incidents. Among them, the Landau–Ginzburg–Higgs (LGH) model is a top-significance model in the modern age. Initially, the LGH model was introduced by Landau and Ginzburg to describe superconductivity and drift cyclotron waves in radially inhomogeneous plasmas of integrated ion cyclotrons.[33] Due to the vast applications of the LGH model, numerous researchers have investigated this model to find the soliton solution using different methods or techniques, such as the first integral scheme,[34] technique of $(G'/G,1/G)$-expansion,[35] technique of Kudryashov,[36] the improved Bernoulli sub-equation function scheme,[37] technique of multi-symplectic Runge–Kutta,[38] new modified simple equation scheme,[39] sine-cosine and extended tanh function technique,[40] inverse scattering transformation technique,[21] and more.

The primary objective of our study is to explore soliton solutions to the nonlinear space–time fractional LGH model,[1] as given in Equation (1).

$$D_{M,t}^{2\alpha,\beta}u - D_{M,x}^{2\alpha,\beta}u - m^2u + n^2u^3 = 0 \tag{1}$$

where $0<\alpha<1, \beta>1$, x and t are the space variable and time variable, respectively, and α and β are the fractional orders of derivatives.

Formerly, the fractional LGH model was handled via some proficient, well-organized, and powerful techniques to investigate different solitary solutions, such asthe methods of $(G'/G,1/G)$-expansion, modified (G'/G^2), and auxiliary equation,[1] the variational iteration transform method,[41] and others. To the best of our knowledge, it has been established that the fractional LGH model has not been investigated utilizing the GERF scheme and the extended tanh-function scheme.

The primary objective of our study is to investigate solitary wave solutions to the fractional LGH model using the two stated methods. The physical significance of the established solutions is illustrated by sketching three-dimensional (3D) and corresponding two-dimensional (2D) plots of the soliton solutions. The established results will be implemented openly to reveal the dynamical behaviors and corporeal implications of the considered model, which will help in solving other fractional models via the GERF and the extended tanh-function scheme.

The remaining part of this article is structured as follows: In Section 2, the explanation of the TMFD is discussed. The GERF and the extended tanh-function scheme are explained in Section 3. In Section 4, the solitary wave solutions to the nonlinear fractional LGH model are extracted. In Section 5, we discuss the dynamical behaviors and physical implications of the established solutions by sketching 3D, along with 2D plots of the solutions. In Section 6, we discuss the novelty of this study. Finally, the article is concluded with concluding remarks.

2. A short note on truncated M-fractional derivative

This segment discusses the features of the TMFD of non-integer order.

Definition: Assume $p:(0,\infty)\to R$, then, the TMFD p of order α is ascertained as shown in Equation (2).

$$D_M^{\alpha,\beta}p(t) = \lim_{\varepsilon\to 0}\frac{p\left(t\epsilon_\beta\left(\varepsilon t^{1-\alpha}\right)\right)-p(t)}{\varepsilon} \tag{2}$$

for every $t>0,\ 0<\alpha<1,\ \beta>0$, where $\alpha\in\beta(\cdot)$ is a truncated Mittag–Leffler function of one parameter.[42]

Features: Consider $\alpha\in(0,\,1],\ \beta>0$ and $p=p(t),\ q=q(t)$ are α-differentiable at a point $t>0$, the subsequent calculation is shown in Equations (3)–(8).

$$D_M^{\alpha,\beta}(ap+bq) = aD_M^{\alpha,\beta}p + bD_M^{\alpha,\beta}q, \tag{3}$$

where $\forall a,b\in R$,

$$D_M^{\alpha,\beta}(c) = 0 \tag{4}$$

where $p(t)=c$, is a constant

$$D_M^{\alpha,\beta}(p\cdot q) = D_M^{\alpha,\beta}p + D_M^{\alpha,\beta}q \tag{5}$$

$$D_M^{\alpha,\beta}\left(\frac{p}{q}\right) = \frac{qD_M^{\alpha,\beta}p + pD_M^{\alpha,\beta}q}{q^2} \tag{6}$$

If p is differentiable, then

$$D_M^{\alpha,\beta}p(t) = \frac{t^{1-\alpha}}{\Gamma(\beta+1)}\frac{dp}{dt} \tag{7}$$

$$D_M^{\alpha,\beta}(p\circ q)(t) = p^{'}(q(t))D_M^{\alpha,\beta}q(t) \tag{8}$$

for p differentiable at $q(t)$

The TMFD is a competent instrument for explaining the characteristics of composite systems of non-integer order derivatives.

3. Displayed algorithm of the employed methods

Here, we discuss the GERF and the extended tanh function technique to establish the solitary wave solutions of the nonlinear fractional LGH model. The universal form of a nonlinear fractional PDE can be written as Equation (9).

$$H\left(u,\ D_t^{\alpha}u,\ D_x^{\beta}u,\ D_y^{\gamma}u,\ D_t^{2\alpha}u\ldots\right) = 0, \tag{9}$$

where the polynomial H involved $u(t,x,y)$ and the partial derivative of u that contain the uppermost order derivatives, linear and nonlinear terms, here $u = u(t,\ x, y)$ is a wave variable function. The subscripts indicate incomplete derivatives.

3.1. A brief description of the generalized exponential rational function method

To get the solution of Equation (9) by using the GERF method, the consequent steps were performed Equations (10)–(14):

Step 1: Let

$$u(x,y,t) = u(\xi) \tag{10}$$

where $\xi = m\frac{x^\beta}{\beta} + n\frac{y^\gamma}{\gamma} \pm k\frac{t^\alpha}{\alpha}$, and k is the velocity parameter. Equation (9) will be transformed to the following ordinary differential equation by using the wave transformation in Equation (10).

$$\mathcal{F}\left(u,\ u^{'},\ u^{''},\ \ldots\right) = 0 \tag{11}$$

where polynomial $\mathcal{F}$contains the term $u(\xi)$ and the differentiation of $u(\xi)$, in which $u^{'}(\xi) = \frac{du}{d\xi}$.

Step 2: The core statement of this technique is the formation of the soliton solution in Equation (11) as follows:

$$u(\xi) = \mathcal{B}_0 + \sum_{i=1}^{N} \mathcal{B}_i f^i(\xi) + \sum_{i=1}^{N} \frac{\mathcal{A}_i}{f^i(\xi)} \tag{12}$$

where

$$f(\xi) = \frac{c_1 e^{(d_1\xi)} + c_2 e^{(d_2\xi)}}{c_3 e^{(d_3\xi)} + c_4 e^{(d_4\xi)}} \tag{13}$$

the constants $c_n, d_n (1 \le n \le 4), \mathcal{B}_0, \mathcal{B}_i$ and $\mathcal{A}_i (1 \le i \le N)$ are ascertained. The structure of the solution in Equation (12) always persuades Equation (11). The score of N will be found using the homogeneous balance principle.

Step 3: Putting Equation (12) into Equation (11) with Equation (13) gives a polynomial Equation (14).

$$S\left(P_1, P_2, P_3, P_4\right) = 0 \tag{14}$$

where $P_j = e^{(d_j\xi)}$ and $j = 1, 2, 3, 4$. A set of nonlinear equations is generated by setting all the coefficients of different powers of ξ to zero.

Step 4: By addressing the set of equations in **Step 3** through utilizing symbolic computation software, such as Mathematica or Maple. The constant $c_n, d_n (1 \le n \le 4)$, $\mathcal{B}_0$, $\mathcal{B}_i$ and $\mathcal{A}_i (1 \le i \le N)$ will can be found. Inserting these results in Equation (12) introduces the soliton solutions of NLEEs.

3.2. A brief description of the extended tanh function method

The extended tanh function method suggests the following steps Equations (15)–(17) to explore the solitary wave solutions of Equation (9).

Step 1: For simplifications, integrate Equation (11) term by term as per possibility and consider the constants of integration as zero.

Step 2: Assume a free variable $Y = \tanh(\mu\xi)$ where:

$$\frac{d}{d\xi} = \mu(1 - Y^2)\frac{d}{dY}. \tag{15}$$

$$\frac{d^2}{d\xi^2} = \mu^2\left(1 - Y^2\right)\left\{\left(1 - Y^2\right)\frac{d^2}{dY^2} - 2Y\frac{d}{dY}\right\}. \tag{16}$$

Step 3: This method suggests the structure of a formal solution of Equation (11) as follows:

$$u(\xi) = \sum_{i=0}^{N} a_i Y^i + \sum_{i=1}^{N} b_i Y^{-i}, \tag{17}$$

where $Y = \tanh(\mu\xi)$ and a_i , b_i are random constants to be evaluated, and the constant $\mu \neq 0$.

Step 4: The positive integer N will be determined by the homogeneous balance principle in Equation (11).

Step 5: Integrating Equation (17) into Equation (11) and setting all the coefficients of different powers of Y to zero, to generate a system equation (algebraic) for $a_0, a_1, a_2, \ldots, a_N,\ b_1, b_2, b_3, \ldots, b_N$ and other random constant. The resulting system is then solved using computer algebra software such as Mathematica or Maple to obtain the parameter values.

Step 6: Setting the results into Equation (17), then the solutions of Equation (11) are found.

4. Solution of the nonlinear space–time fractional Landau–Ginzburg–Higgs model

This segment investigates the nonlinear space-time fractional LGH model to explore several newer, functional, and competent solitary wave solutions of the model using the considered methods. Now, we have examined the nonlinear fractional LGH model in Equation (1). Let

$$u(\xi) = u(t,x,y),$$

where $\xi = \frac{\Gamma(\beta+1)}{\alpha}\left(kx^\alpha - \omega t^\alpha\right)$, and k and ω are constant. Using the transformation from Equation (1), we acquire the subsequent nonlinear ordinary differential equation as shown in Equation (18).

$$\left(\omega^2 - k^2\right)u^{''} - m^2 u + n^2 u^3 = 0 \tag{18}$$

4.1. Soliton solution using the generalized exponential rational function method

Applying the homogeneous balance principle between the utmost order nonlinear and linear terms arises in Equation (18) and get $N = 1$. As a result, the structure of the solution of Equation (18) can be written as Equation (19).

$$u(\xi) = a_0 + a_1 f(\xi) + \frac{b_1}{f(\xi)}, \tag{19}$$

By applying the necessary sequences of this technique, the solutions of the model are found as the following sets and equations Equations (20)–(44):

Set 1: Assume $c = [-3, -2, 1, 1]\ and\ d = [0, 1, 0, 1]$

$$f(\xi) = \frac{-3 - 2e^\xi}{1 + e^\xi} \tag{20}$$

Case 1.1: When $\omega = \pm\sqrt{(k^2 - 2m^2)}, a_0 = -\frac{5m}{n}, a_1 = 0, b_1 = -\frac{12m}{n}$, our achieved solution:

$$u(x,t) = -\frac{m}{n}\left(5 - 12\left(\frac{1 + e^{\left(\frac{\Gamma(\beta+1)}{\alpha}(kx^\alpha - \omega t^\alpha)\right)}}{3 + 2e^{\left(\frac{\Gamma(\beta+1)}{\alpha}(kx^\alpha - \omega t^\alpha)\right)}}\right)\right) \tag{21}$$

Set 2: Assume $c = [-2, 0, -1, 1]\ and\ d = [1, -1, 1, -1]$

$$f(\xi) = \frac{\cos h(\xi) + sinh(\xi)}{\sin h(\xi)} \tag{22}$$

Case 2.1: If $\omega = \pm\frac{\sqrt{\left(4k^2-2m^2\right)}}{2}, a_0 = \frac{m}{n}, a_1 = -\frac{m}{n}, b_1 = 0$, our achieved solution:

$$u(x,t) = \frac{m}{n}\left(-coth\left(\frac{\Gamma(\beta+1)}{\alpha}\left(kx^{\alpha} - \omega t^{\alpha}\right)\right)\right) \tag{23}$$

Set 3: Consider $c = [1-i, -1-i, -1, 1]$ *and* $d = [i, -i, i, -i]$

$$f(\xi) = \frac{\cos(\xi) - \sin(\xi)}{sin(\xi)} \tag{24}$$

Case 3.1: When $\omega = \pm\frac{\sqrt{\left(4k^2+2m^2\right)}}{2}, a_0 = \pm i\frac{m}{n}, a_1 = \pm i\frac{m}{n}, b_1 = 0$, we get the soliton solution:

$$u(x,t) = \pm i\frac{m}{n}\left(1 + cot\left(\frac{\Gamma(\beta+1)}{\alpha}\left(kx^{\alpha} - \omega t^{\alpha}\right)\right)\right) \tag{25}$$

Set 4: Assume $c = [2-i, -2-i, -1, 1]$ *and* $d = [i, -i, i, -i]$

$$f(\xi) = \frac{-2sin(\xi) + \cos(\xi)}{sin(\xi)} \tag{26}$$

Case 4.1: When $\omega = \pm\frac{\sqrt{\left(4k^2+2m^2\right)}}{2}, a_0 = \pm i\frac{2m}{n}, a_1 = \pm i\frac{m}{n}, b_1 = 0$, our achieved solution:

$$u(x,t) = \pm i\frac{m}{n}\left(\tan\left(\frac{\Gamma(\beta+1)}{\alpha}\left(kx^{\alpha} - \omega t^{\alpha}\right)\right)\right) \tag{27}$$

Set 5: Let $c = [2, 1, 1, 1]$ *and* $d = [1, 0, 1, 0]$

$$f(\xi) = \frac{2e^{\xi} + 1}{e^{\xi} + 1} \tag{28}$$

Case 5.1: When $\omega = \pm\sqrt{(k^2 - 2m^2)}, a_0 = -\frac{3m}{n}, a_1 = 0, b_1 = \frac{4m}{n}$, we get the soliton solution:

$$u(x,t) = -\frac{m}{n}\left(3 - 4\left(\frac{e^{\left(\frac{\Gamma(\beta+1)}{\alpha}(kx^{\alpha} - \omega t^{\alpha})\right)} + 1}{2e^{\left(\frac{\Gamma(\beta+1)}{\alpha}(kx^{\alpha} - \omega t^{\alpha})\right)} + 1}\right)\right) \tag{29}$$

Set 6: Let $c = [-1, 0, 1, 1]$ *and* $d = [0, 1, 0, 1]$

$$f(\xi) = -\frac{1}{e^{\xi} + 1} \tag{30}$$

Case 6.1: When $\omega = \pm\sqrt{(k^2 - 2m^2)}, a_0 = \frac{m}{n}, a_1 = \frac{2m}{n}, b_1 = 0$, our achieved solution:

$$u(x,t) = \frac{m}{n}\left(1 - 2\left(\frac{1}{e^{\left(\frac{\Gamma(\beta+1)}{\alpha}(kx^{\alpha} - \omega t^{\alpha})\right)} + 1}\right)\right) \tag{31}$$

Set 7: Consider $c = [-1, -1, 1, -1]$ *and* $d = [1, -1, 1, -1]$

$$f(\xi) = -\frac{\cos h(\xi)}{\sin h(\xi)} \tag{32}$$

Case 7.1: When $\omega = \pm\frac{\sqrt{\left(4k^2+m^2\right)}}{2}a_0 = 0, a_1 = \pm i\frac{m}{n\sqrt{2}}, b_1 = \pm i\frac{m}{n\sqrt{2}}$, our achieved solution:

$$u(x,t) = \pm i\frac{m}{n\sqrt{2}}\left(\tan h\left(\frac{\Gamma(\beta+1)}{\alpha}\left(kx^{\alpha} - \omega t^{\alpha}\right)\right)\right. \\ \left. - \coth\left(\frac{\Gamma(\beta+1)}{\alpha}\left(kx^{\alpha} - \omega t^{\alpha}\right)\right)\right. \tag{33}$$

Set 8: Assume $c = [-1-i, 1-i, -1, 1]$ *and* $d = [i, -i, i, -i]$

$$f(\xi) = \frac{\sin(\xi) + \cos(\xi)}{sin(\xi)} \tag{34}$$

Case 8.1: When $\omega = \pm\frac{\sqrt{\left(4k^2+2m^2\right)}}{2}, a_0 = \mp i\frac{m}{n}, a_1 = 0, b_1 = \pm i\frac{2m}{n}$, our achieved solution:

$$u(x,t) = \\ \mp i\frac{m}{n}\left(1 - \frac{2sin\left(\frac{\Gamma(\beta+1)}{\alpha}\left(kx^{\alpha} - \omega t^{\alpha}\right)\right)}{\left(\cos\left(\frac{\Gamma(\beta+1)}{\alpha}\left(kx^{\alpha} - \omega t^{\alpha}\right)\right) + sin\left(\frac{\Gamma(\beta+1)}{\alpha}\left(kx^{\alpha} - \omega t^{\alpha}\right)\right)\right)}\right). \tag{35}$$

Set 9: Let $c = [-2-i, 2-i, -1, 1]$ *and* $d = [1, -1, 1, -1]$

$$f(\xi) = \frac{\cos(\xi) + 2sin(\xi)}{sin(\xi)} \tag{36}$$

Case 9.1: When $\omega = \pm\frac{\sqrt{\left(4k^2+2m^2\right)}}{2}, a_0 = \mp i\frac{2m}{n}, a_1 = 0, b_1 = \pm i\frac{5m}{n}$, we arrive at the soliton solution:

$$u(x,t) = \\ \mp i\frac{m}{n}\left(2 - \frac{5sin\left(\frac{\Gamma(\beta+1)}{\alpha}\left(kx^{\alpha} - \omega t^{\alpha}\right)\right)}{\left(\cos\left(\frac{\Gamma(\beta+1)}{\alpha}\left(kx^{\alpha} - \omega t^{\alpha}\right)\right) + 2sin\left(\frac{\Gamma(\beta+1)}{\alpha}\left(kx^{\alpha} - \omega t^{\alpha}\right)\right)\right)}\right) \tag{37}$$

Set 10: Suppose $c = [4, 0, 4, 4]$ *and* $d = [4, -4, 4, 0]$

$$f(\xi) = \frac{e^{4\xi}}{1 + e^{4\xi}} \tag{38}$$

Case 10.1: When $\omega = \pm\frac{\sqrt{\left(16k^2-2m^2\right)}}{4}, a_0 = \frac{m}{n}, a_1 = -\frac{2m}{n}, b_1 = 0$, our achieved solution:

$$u(x,t) = \frac{m}{n}\left(1 - 2\left(\frac{e^{4\left(\frac{\Gamma(\beta+1)}{\alpha}(kx^{\alpha} - \omega t^{\alpha})\right)}}{1 + e^{4\left(\frac{\Gamma(\beta+1)}{\alpha}(kx^{\alpha} - \omega t^{\alpha})\right)}}\right)\right) \tag{39}$$

Set 11: Assume $c = [-1, -2, 1, 1]$ *and* $d = [1, 0, 1, 0]$

$$f(\xi) = \frac{-e^{\xi} - 2}{e^{\xi} + 1} \tag{40}$$

Case 11.1: When $\omega = \pm\sqrt{(k^2 - 2m^2)}, a_0 = -\frac{3m}{n}, a_1 = -\frac{2m}{n}, b_1 = 0$, we arrive at the soliton solution:

$$u(x,t) = \\ -\frac{m}{n}\left(3 - 2\left(\frac{e^{\left(\frac{\Gamma(\beta+1)}{\alpha}(kx^{\alpha} - \omega t^{\alpha})\right)} + 2}{e^{\left(\frac{\Gamma(\beta+1)}{\alpha}(kx^{\alpha} - \omega t^{\alpha})\right)} + 1}\right)\right) \tag{4.24}$$

Set 12: Assume $c = [1, -3, -1, 1]$ *and* $d = [1, -1, 1, -1]$

$$f(\xi) = \frac{\cos h(\xi) - 2sinh(\xi)}{\sin h(\xi)} \tag{41}$$

Case 12.1: When $\omega = \pm\frac{\sqrt{\left(4k^2-2m^2\right)}}{2}, a_0 = \frac{2m}{n}, a_1 = \frac{m}{n}, b_1 = 0$, our achieved solution:

$$u(x,t) = \frac{m}{n}\left(\tan h\left(\frac{\Gamma(\beta+1)}{\alpha}\left(kx^{\alpha} - \omega t^{\alpha}\right)\right)\right) \tag{42}$$

Set 13: Let $c = [3, 2, 1, 1]$ *and* $d = [1, 0, 1, 0]$

$$f(\xi) = \frac{3e^{\xi} + 2}{e^{\xi} + 1} \tag{43}$$

Case 13.1: When $\omega = \pm\sqrt{(k^2 - 2m^2)}, a_0 = \frac{5m}{n}, a_1 = -\frac{2m}{n}, b_1 = 0$, we arrive at the soliton solution:

$$u(x,t)=\frac{m}{n}\left(5-2\left(\frac{3e^{\left(\frac{\Gamma(\beta+1)}{\alpha}(kx^{\alpha}-\omega t^{\alpha})\right)}+2}{e^{\left(\frac{\Gamma(\beta+1)}{\alpha}(kx^{\alpha}-\omega t^{\alpha})\right)}+1}\right)\right) \quad (44)$$

It is remarkable to note that the soliton solutions of the considered model are comprehensive, novel, and useful, which are not found in previous studies.

4.2. Soliton solution via the extended tanh-function method

Proceeding with the above procedure, we get $N = 1$. Consequently, the solution structures of Equation (18) are as follows Equations (45) and (46):

$$u(\xi)=a_0+a_1Y(\xi)+\frac{b_1}{Y(\xi)}, \quad (45)$$

where $Y(\xi)=\tanh(\xi)$

By using the necessary sequences of this technique, the solutions of the model are given below:

$$\omega=\pm\frac{\sqrt{(4k^2-2n^2l^2)}}{2}, \mathrm{a}_0=0, a_1=\tfrac{m^2}{3ln^2}, b_1=l$$

where l is an arbitrary constant.

Our achieved solution:

$$\begin{aligned}u(x,t)&=\frac{m^2}{3ln^2}\tan h\left(\frac{\Gamma(\beta+1)}{\alpha}\left(kx^{\alpha}+\omega t^{\alpha}\right)\right)\\&+lcoth\left(\frac{\Gamma(\beta+1)}{\alpha}\left(kx^{\alpha}+\omega t^{\alpha}\right)\right)\end{aligned} \quad (46)$$

It is remarkable to state that the obtained soliton solution of the nonlinear fractional LGH model is further general, newer, and useful than those in the earlier study.

5. Graphical illustration and physical implications of the outcome

This segment explains the physical importance of the established soliton solutions. The primary aim of this 3D and combined 2D graphical representation is to describe the dynamic characteristics of the obtained soliton solutions for small changes in the velocity parameter inside a suitable time interval. For simplicity, we confer the solutions of Equations (21), (25), (29), (31), (33), (39), (42), and (46), and the remaining results are presented here. The effect of the velocity parameter on solitons is examined as shown in Figure 1.

The soliton of Equation (21) displays multiple periodic solitons for the velocity parameter $\omega = 2.00,\ 1.90,$ and 1.80, correspondingly (Figure 1A–C). It was found that the 3D shapes changed with the decrease of ω. Figure 1D shows the 2D united plot of Equation (21), which shows the influence of the velocity parameter ω on the solitons by keeping other involved parameters unchanged.

Again, the solution of Equation (25) exhibits multiple periodic solitons for the velocity parameter $\omega = 1.40,\ 1.15,$ and 0.90, respectively (Figure 2A–C). The 3D shape is changing with the change of ω, and Figure 2D shows the 2D combined plot of Equation (25).

Moreover, the solution of Equation (29) displays a bell-shaped soliton for $\omega = 0.90,\ 0.80,$ and 0.70, respectively (Figure 3A–C). The shape of 3D graphs varies with ω varies. Figure 3D shows the 2D combined graphs of Equation (29).

Again, the solution of Equation (31) shows the periodic soliton for $\omega = 2.50,\ 3.00,$ and 3.50, correspondingly (Figure 4A–C). The shape of the 3D plot changes with the changes in ω. Figure 4D shows the 2D combined graph of Equation (31).

Similarly, the solution of Equation (33) displays multiple singular periodic solitons for $\omega = 1.60,\ 1.33,$ and 1.17, correspondingly (Figure 5A–C). The shape of the 3D plot changes with the changes in ω. Figure 5D displays the 2D combined plot of Equation (33).

Here, Equation (39) shows multiple periodic solitons for $\omega = 1.35,\ 1.15,$ and 0.80, correspondingly (Figure 6A–C). The shape of the 3D design changes with the change of ω. Figure 6D shows a 2D combined plot of Equation (39).

The solution Equation (42) shows the multiple periodic soliton for $\omega = 2.00,\ 1.50,$ and 1.00, respectively (Figure 7A–C). The shape of the 3D plot changes with the change of ω. Figure 7D displays the 2D combined diagram of Equation (42).

Equation (46) shows multiple periodic solitons for velocity parameters $\omega = 2.48,\ 1.25,$ and 0.41, respectively (Figure 8A–C). The shape of the 3D figures varies with the variation of the velocity parameter ω varies. Figure 8D shows the 2D combined plot of Equation (46).

From Figures 1–8, it is clear that the behavior of wave propagation related to the model is significantly influenced by the velocity parameter. The similar solution represents diverse characteristics for the different values wave velocity parameter. It is observed that the obtained solutions display some familiar 3D structures, such as multiple singular periodic solitons, multiple periodic solitons, kink waves, spike shapes, bell-shaped solitons, etc. We have found different types of soliton solutions that are exponential, trigonometric, compound hyperbolic, hyperbolic, and their combination.

6. The novelty of established results

Zulqarnain et al.[1] investigated the fractional LGH model using $\left(\frac{G'}{G^2}\right)$ -expansion method. The outcome of their study shows notable differences in the methodology, objectives, outcome, and contributions from our work. This comparison intends to scrutinize these distinctions to highlight the novelty and superiority of our study.

(i) Utilized techniques: This study utilized a novel solution technique, the GERF technique, and the extended tanh-function technique. In contrast, Zulqarnain et al.[1] utilized the comparatively elderly solution technique, which limits the scope of analytical exploration.

(ii) Soliton structure: Our investigation produced different types of familiar soliton structures, such as singular periodic shapes, continuous periodic shapes, bell-shaped waves, and singular kink shapes. This is a better assortment of coherent structures compared to the study conducted by Zulqarnain et al.[1] Additionally, their study only showed limited types of familiar soliton structures, such as singular periodic solitons. This showed a narrower assortment of wave shape.

(iii) Corporeal insights: This study shows deeper insights into solitary wave dynamics employing two recently introduced methods. On the other hand, Zulqarnain et al.[1] provided an inadequate explanation of results and their corporeal meanings.

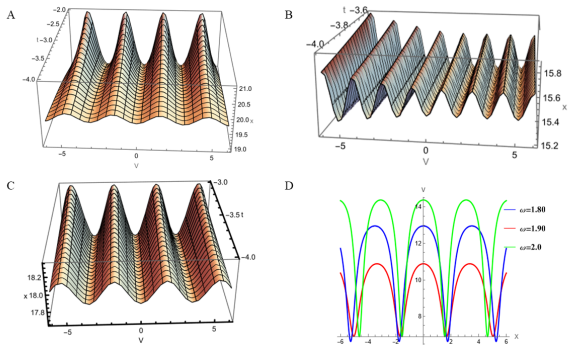

Figure 1. Solitonic structure of the solution of Equation (21). (A) The three-dimensional design for $\omega = 2.50$. (B) The three-dimensional design for $\omega = 1.90$. (C) The three-dimensional design for $\omega = 1.80$. (D) The two-dimensional united plot.

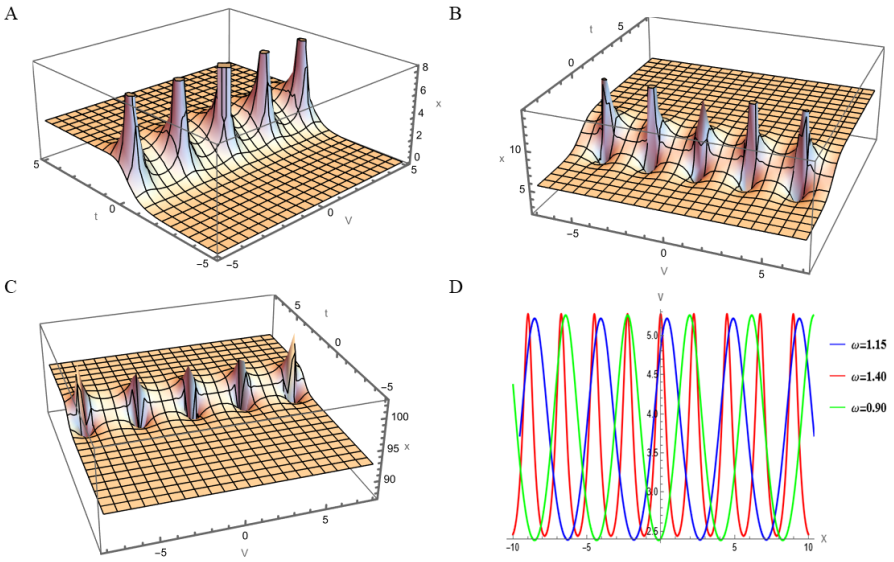

Figure 2. Solitonic structure of Equation (25). (A) The three-dimensional design for $\omega = 1.00$. (B) The three-dimensional design for $\omega = 1.15$. (C) The three-dimensional design for $\omega = 0.90$. (D) The two-dimensional united plot.

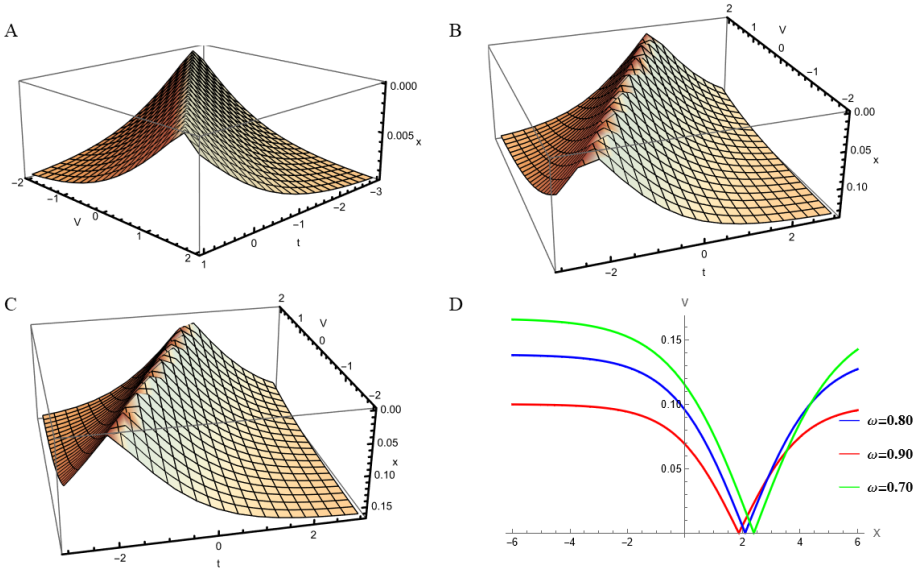

Figure 3. Solitonic structure of Equation (29). (A) The three-dimensional design for $\omega = 0.90$. (B) The three-dimensional design for $\omega = 0.80$. (C) The three-dimensional design for $\omega = 0.70$. (D) The two-dimensional united plot.

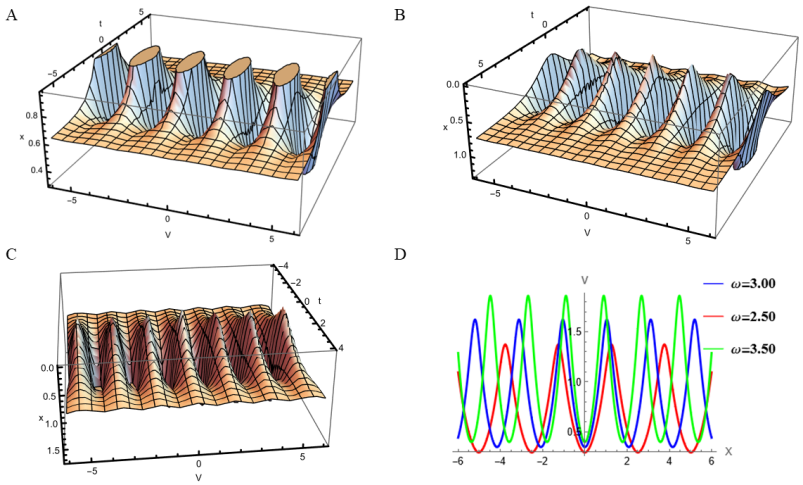

Figure 4. Solitonic structure of the solution of Equation (31). (A) The three-dimensional design for $\omega = 2.50$. (B) The three-dimensional design for $\omega = 3.00$. (C) The three-dimensional design for $\omega = 3.50$. (D) The two-dimensional united plot.

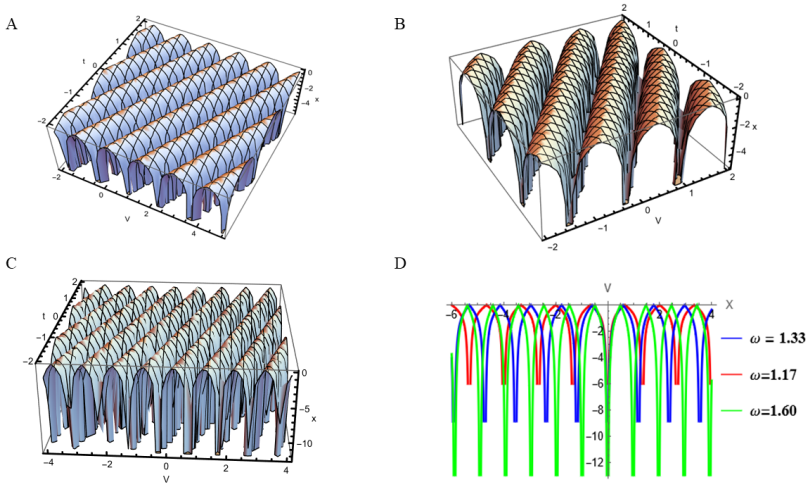

Figure 5. Solitonic structure of Equation (33). (A) The three-dimensional design for $\omega = 1.60$. (B) The three-dimensional design for $\omega = 1.33$. (C) The three-dimensional design for $\omega = 1.17$. (D) The two-dimensional united plot.

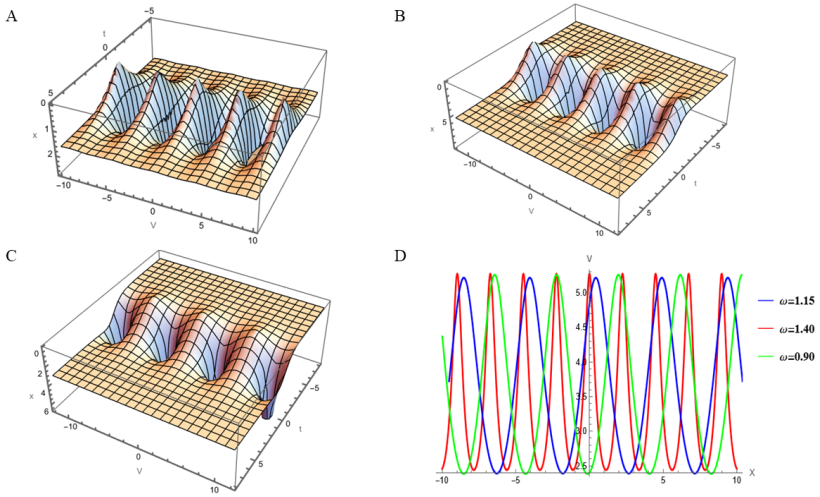

Figure 6. Solitonic structure of Equation (39). (A) The three-dimensional design for $\omega = 1.35$. (B) The three-dimensional design for $\omega = 1.50$. (C) The three-dimensional design for $\omega = 0.80$. (D) The two-dimensional united plot.

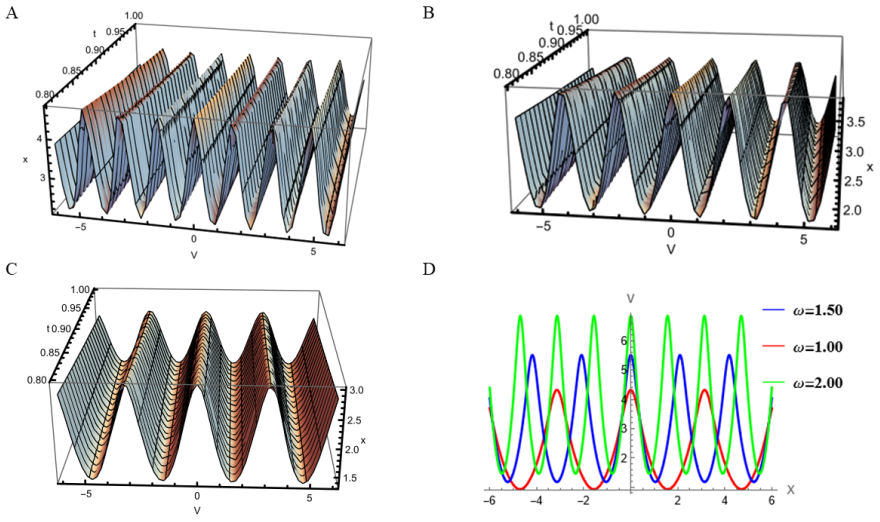

Figure 7. Solitonic structure of Equation (42). (A) The three-dimensional design for $\omega = 2.00$. (B) The three-dimensional design for $\omega = 1.50$. (C) The three-dimensional design for $\omega = 1.00$. (D) The two-dimensional united plot.

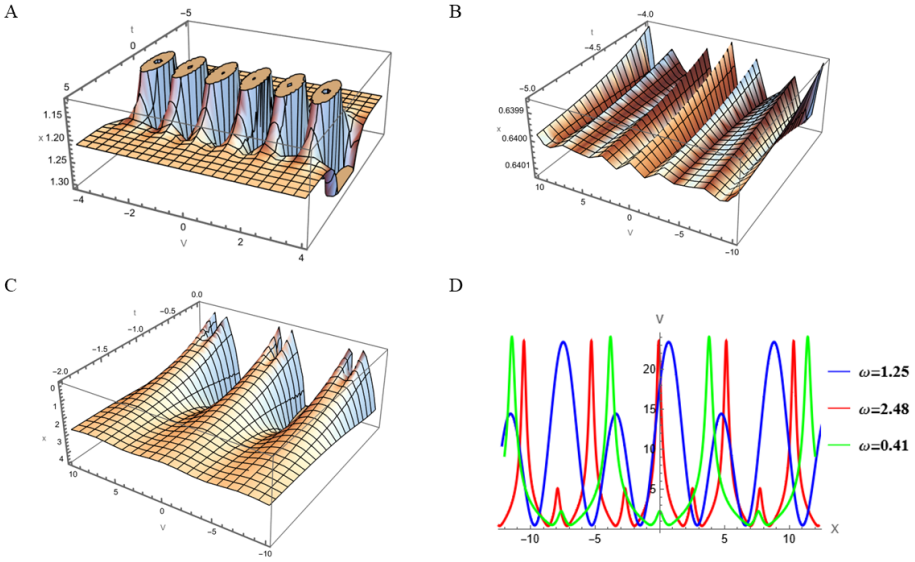

Figure 8. Solitonic structure of Equation (46). (A) The three-dimensional design for $\omega = 2.48$. (B) The three-dimensional design for $\omega = 1.25$. (C) The three-dimensional design for $\omega = 0.41$. (D) The two-dimensional united plot.

(iv) Contributions: This study notably increases the perceptive of nonlinear wave evolution. In contrast, Zulqarnain et al.[1] showed inadequate novel knowledge.

In summary, this study represents a more inclusive, rigorous, and innovative investigation of the LGH model by employing a wider range of advanced analytical techniques. It yields novel insights and offerssuperior contributions to the field of nonlinear wave study compared to the study performed by Zulqarnain et al.[1]

7. Conclusion

In this article, the GERF method and the extended tanh-function method have been efficiently applied to explore solitary wave solutions to the fractional order LGH model by means of the TMFD. The pictographic representation exhibits the dynamic behavior of the attained solutions and gives diverse structures of graphs, such as multiple periodic solitons, multiple singular periodic solitons, kink waves, spike shapes, and bell-shaped solitons. This study shows that the value of the wave velocity parameter influences the signal transmission related to the nonlinear fractional LGH model. Correctness of attained solutions was confirmed by incorporating them into the considered model with the aid of the Maple program, and the results were accurate. This suggests that the GERF method and extended tanh-function method are efficient and straightforward, exhibiting easily implementable characteristics for exploring a wide range of soliton solutions of nonlinear fractional differential equations. Our established solution can support the analysis of the inner mechanism of physical incidents connected with superconductivity, plasma physics, geo-optical filaments, and numerous engineering applications. Due to the outstanding performance of the GERF method and the extended tanh-function method, various important models

can be investigated using these methods. However, the extended tanh-function method provides a limited number of soliton solutions.

Acknowledgments

None.

Funding

None.

Conflict of interest

The authors declare they have no competing interests.

Author contributions

Conceptualization: M. Al Amin
Formal analysis: M. Al Amin
Investigation: M. Al Amin
Methodology: M. Al Amin
Software: M. Al Amin
Supervision: M. Nurul Islam, M. Ali Akbar
Validation: M. Al Amin
Writing–original draft: M. Al Amin
Writing–review & editing: M. Nurul Islam, M. Ali Akbar

Availability of data

No datasets were generated or analyzed during the current study.

AI Tools Statement

We confirm that no AI tools were used in the preparation of this manuscript.

References

1. Zulqarnain RM, Ma WX, Mehdi KB, Siddique I, Hassan AM, Askar, S. Physically significant solitary wave solutions to the space-time fractional Landau-Ginsburg-Higgs equation via three consistent methods. *Front Phys.* 2023;11:1205060. https://doi.org/10.3389/fphy.2023.1205060
2. Gómez-Aguilar JF, Baleanu D. Schrödinger equation involving fractional operators with non-singular kernel. *J Electromagn Waves Appl.* 2017;31(7):752-761. https://doi.org/10.1080/09205071.2017.1312556
3. Hosseini K, Mirzazadehm M, Gómez-Aguilar JF. Soliton solutions of the Sasa-Satsuma equation in the monomode optical fibers including the beta-derivatives. *Optik.* 2020;224:165425. https://doi.org/10.1016/j.ijleo.2020.165425
4. Khalil R, Horani MA, Yousef A, Sababheh M. A new definition of fractional derivative. *J Comput Appl Math.* 2014;264:65-70. https://doi.org/10.1016/j.cam.2014.01.002
5. Al-Amin M, Islam MN. Mathematical analysis and study of the numerous traveling wave behavior for different wave velocities of the soliton solutions for the nonlinear Landau-Ginsberg-Higgs model in nonlinear media. *J Mech Cont Math Sci.* 2023;18(7), 24-37. https://doi.org/10.26782/jmcms.2023.07.00003
6. Akinyemi L, Houwe A, Abbagari S, Wazwaz AM, Alshehri HM, Osman MS. Effects of the higher-order dispersion on solitary waves and modulation instability in a monomode fiber. *Optik.* 2023;288(1):171202. https://doi.org/10.1016/j.ijleo.2023.171202
7. Al-Amin M, Islam MN, Ilhan OA, Akbar MA, Soybas D. Solitary wave solutions to the modified Zakharov-Kuznetsov and the (2+1)-dimensional Calogero-Bogoyavlenskii-Schiff models in mathematical physics. *J Math.* 2022;2022:5224289. https://doi.org/10.1155/2022/5224289
8. Rahman RU, Hammouch Z, Alsubaie ASA, Mahmoud KH, Alshehri A, Az-Zo'bi EA, Osman MS. Dynamical behavior of fractional nonlinear dispersive equation in Murnaghan's rod materials. *Results Phys.* 2024;56:107207. https://doi.org/10.1016/j.rinp.2023.107207
9. Al-Amin M, Islam MN, Akbar MA. Abundant exact soliton solutions to the space-time fractional Phi-Four effective model for quantum effects through the modern scheme. *Int J Sci Basic Appl Res.* 2021;60(4):1-16.
10. Razzaq W, Habib M, Nadeem M, Zafar A, Khan I, Mwanakatwea PK. Solitary wave solutions of conformable time fractional equations using modified simplest equation method. *Complexity.* 2022;9:8705388. https://doi.org/10.1155/2022/8705388
11. Rahman HU, Yasin S, Iqbal I. Optical soliton for (2+1)-dimensional coupled integrable NLSE using Sardar-sub-equation method. *Mod Phys Lett B.* 2024;38(10):2450044. https://doi.org/10.1142/S0217984924500441
12. Yang JY, Ma WX, Khalique CM. Determining lump solutions for a combined soliton equation in (2+1)-dimensions. *Eur Phys J Plus.* 2020;135:494(2020). https://doi.org/10.1140/epjp/s13360-020-00463-z
13. Ma WX. N-soliton solutions and the Hirota conditions in (2+1)-dimensions. *Opt Quantum Electron.* 2020;52:511. https://doi.org/10.1007/s11082-020-02628-7
14. Ma WX. N-soliton solution and the Hirota condition of a (2+1)-dimensional combined equation. *Math Comput Simul.* 2021;190:270-279. https://doi.org/10.1016/j.matcom.2021.05.020
15. Ma WX. N-soliton solutions and the Hirota conditions in (1+1)-dimensions. *Int J Nonlinear Sci Numer Simul.* 2022;23(1):123-133. https://doi.org/10.1515/ijnsns-2020-0214
16. Ma WX, Yong X, Lü X. Soliton solutions to the B-type Kadomtsev-Petviashvili equation under general dispersion relations. *Wave Motion.* 2021;103:102719. https://doi.org/10.1016/j.wavemoti.2021.102719
17. Al-Amin M, Islam MN, Akbar MA. Adequate wide-ranging closed-form wave solutions to a nonlinear biological model. *Partial Differ Equ Appl Math.* 2021;4:100042. https://doi.org/10.1016/j.padiff.2021.100042
18. Zafar A, Shakeel M, Ali A, Rezazadeh HH, Brkir A. Analytical study of complex Ginzburg-Landau equation arising in nonlinear optics. *J Nonlinear Opt Phys Mater.* 2023;32(1):2350010. https://doi.org/10.1142/S0218863523500108
19. Arshed S, Akram G, Sadaf M, Shadab H. New traveling wave solutions for paraxial wave equation via two integrating techniques. *Opt Quant Electron.* 2024;56:791. https://doi.org/10.1007/s11082-024-06589-z
20. Hossain MN, Miah MM, Ganie AH, Osman MS, Ma WX. Discovering new abundant optical solutions for the resonant nonlinear Schrödinger equation using an analytical technique. *Opt Quant Electron.* 2024;56:847. https://doi.org/10.1007/s11082-024-06351-5
21. Ali MR, Khattab MA, Mabrouk SM. Travelling wave solution for the Landau-Ginburg-Higgs model via the inverse scattering transformation method. *Nonlinear Dyn.* 2023;111:7687-7697. https://doi.org/10.1007/s11071-022-08224-6
22. Faridi WA, Myrzakulova Z, Myrzakulov R, Akgül A, Osman MS. The construction of exact solution and explicit propagating optical soliton waves of Kuralay equation by the new extended direct algebraic and Nucci's reduction techniques. *Int J Mod Simul.* 2024:1-20. https://doi.org/10.1080/02286203.2024.2315278
23. Alaroud M. Application of Laplace residual power series method for approximate solutions of fractional IVP's. *Alex Eng J.* 2022;61(2):1585-1595. https://doi.org/10.1016/j.aej.2021.06.065
24. Mirzazadeh M, Akbulut A, Taşcan F, Akinyemi L. A novel integration approach to study the perturbed Biswas-Milovic

equation with Kudryashov's law of refractive index. *Optik.* 2022;252:168529. https://doi.org/10.1016/j.ijleo.2021.168529
25. Islam Z, Abdeljabbar A, Sheikh MAN, Roshid HO, Taher MA. Optical solitons to the fractional order nonlinear complex model for wave packet envelope. *Results Phys.* 2022;43:106095. https://doi.org/10.1016/j.rinp.2022.106095
26. Zafar A, Raheel M, Tariq KU, et al. A variety of optical wave solutions to space-time fractional perturbed Kundu-Eckhaus model with full non-linearity. *Opt Quant Electron.* 2024;56:401. https://doi.org/10.1007/s11082-023-06053-4
27. Khater MMA. Dynamics of nonlinear time fractional equations in shallow water waves. *Int J Theor Phys.* 2024;63:92. https://doi.org/10.1007/s10773-024-05634-7
28. Tariq KU, Bekir A, Zubair M. On some new travelling wave structures to the (3+1)-dimensional Boiti-Leon-Manna-Pempinelli model. *J Ocean Eng Sci.* 2024:9(2):99-111. https://doi.org/10.1016/j.joes.2022.03.015
29. Roy R, Akbar MA, Seadawy AR, Baleanu D. Search for adequate closed form wave solutions to space-time fractional nonlinear equations. *Partial Differ Equ Appl Math.* 2021;4:100025. https://doi.org/10.1016/j.padiff.2021.100025
30. Al-Amin M, Islam MN, Akbar MA, Wazwaz AM, Osman MS. Assorted optical soliton solutions of the nonlinear fractional model in optical fibers possessing beta derivative. *Phys Scr.* 2024;99(1):015227. https://doi.org/10.1088/1402-4896/ad1455
31. Ma WX, Zhang Y, Tang Y. Symbolic computation of lump solutions to a combined equation involving three types of nonlinear terms. *East Asian J Appl Math.* 2020;10(4):732-745. https://doi.org/10.4208/eajam.151019.110420%20
32. Ma WX. A novel kind of reduced integrable matrix mKdV equations and their binary Darboux transformations. *Mod Phys Lett B.* 2022;36(20):2250094. https://doi.org/10.1142/S0217984922500944
33. Cyrot M. Ginzburg-Landau theory for superconductors. *Rep Prog Phys.* 1973;36(2):103-158. https://doi.org/10.1088/0034-4885/36/2/001
34. Bekir A, Unsal O. Exact solutions for a class of nonlinear wave equations by using the first integral method. *Int J Nonlinear Sci.* 2013;15(2):99-110.
35. Iftikhar A, Ghafoor A, Jubair T, Firdous S, Mohyud-Din ST. The expansion method for travelling wave solutions of (2+1)-dimensional generalized KdV sine Gordon and Landau-Ginzburg-Higgs equation. *Sci Res Essays.* 2013;8(28):1349-1359. https://doi.org/10.5897/SRE2013.5555
36. Barman HK, Akbar MA, Osman MS, et al. Solutions to the Konopelchenko-Dubrovsky equation and the Landau-Ginzburg-Higgs equation via the generalized Kudryashov technique. *Results Phys.* 2021;24:104092. https://doi.org/10.1016/j.rinp.2021.104092
37. Islam ME, Akbar MA. Stable wave solutions to the Landau-Ginzburg-Higgs equation and the modified equal width wave equation using the IBSEF method. *Arab J Basic Appl Sci.* 2020;27(1):270-278. https://doi.org/10.1080/25765299.2020.1791466
38. Hu WP, Deng ZC, Han SM, Fa W. Multi symplectic Runge-Kutta method for Landau-Ginzburg-Higgs equation. *Appl Math Mech.* 2009;30(8):1027-1034. https://doi.org/10.1007/s10483-009-0809-x
39. Irshad A, Mohyud-Din ST, Ahmed N, Khan U. A new modification in simple equation method and its applications on nonlinear equations of physical nature. *Results Phys.* 2017;7:4232-4240. https://doi.org/10.1016/j.rinp.2017.10.048
40. Cevikel AC, Aksoy E, Guner O, Bekir A. Dark bright soliton solutions for some evolution equations. *Int J Nonlin Sci.* 2013;16(3):195-202.
41. Deng SX, Ge XX. Analytical solution to local fractional Landau-Ginzburg-Higgs equation on fractal media. *Therm Sci.* 2021;25(6B):4449-4455. https://doi.org/10.2298/TSCI2106449D
42. Vanterler D, Sousa JC, de Oliveira EC. A new truncated M-fractional derivative type unifying some fractional derivative types with classical properties. *Int J Anal Appl.* 2018;16(1): 83-96.